

Contents lists available at ScienceDirect

Radiation Physics and Chemistry

journal homepage: www.elsevier.com/locate/radphyschem





Luminescence dating and firing temperature determination of ancient ceramics fragments from the Tunata-hill site in the Churajon archaeological complex in Arequipa, Peru

Yolanda Pacompia ^a, Justo G. Supo-Ramos ^a, Carlos D. Gonzales-Lorenzo ^{a,b,*}, Darwin J. Callo-Escobar ^a, René R. Rocca ^c, Elizabeth C. Pastrana ^d, Monise B. Gomes ^e, Betzabel N. Silva-Carrera ^e, S. Watanabe ^b, Oscar Ayca-Gallegos ^f, Jorge S. Ayala-Arenas ^a

- ^a Universidad Nacional de San Agustín de Arequipa, Av. Independencia S/N, Arequipa, Peru
- ^b Instituto de Física, Universidade de São Paulo, São Paulo, SP, Brazil
- ^c Instituto do Mar, Universidade Federal de São Paulo, Santos, SP, Brazil
- d Facultad de Ciencias, Universidad Nacional de Ingeniería, Lima, Peru
- e Instituto de Pesquisas Energéticas e Nucleares, IPEN-CNEN/SP, Av. Prof. Lineu Prestes, 2242, Cidade Universitária, São Paulo, SP, Brazil
- f Universidad Nacional Jorge Basadre Grohmann, Miraflores S/N, Tacna, Peru

ARTICLE INFO

Keywords:
Dating
Firing temperature
TL
OSL
XRF
Churajon
Tunata-hill

ABSTRACT

Ancient pottery fragments from the Tunata-hill site in Churajon archaeological complex, Arequipa, Peru, were dated by means of luminescence techniques such as thermoluminescence (TL) and optically stimulated luminescence (OSL) in order to provide absolute chronology. For TL, additive and regenerative methods were performed. For OSL a regenerative method was carried out for IRSL dating. A rigorous description of the study area and its context has been made. The ages of the samples were found to be between 0.50 ± 0.06 ky and 0.49 ± 0.03 ky for TL methods, and 0.49 ± 0.02 ky for OSL methods. On average, the estimated age by TL and OSL techniques is 490 ± 70 yr (1600 AD and 1460 AD). This means that Churajon ceramics under study would belong to the Late periods which corresponds to the Inca region, and the North sub-region of the Late Churajon phase, and the beginning of European colonization in Peru. X-ray fluorescence technique (XRF) analysis has shown the main presence of Fe (39.5%), Si (30.0%), and Al (10.4%) in fine pottery powder. Furthermore, the electron paramagnetic resonance (EPR) technique was used to study the firing temperature using the iron signal (Fe³+) as a firing temperature reference. The firing temperature of ceramics was found to be around 550 \pm 50 °C.

1. Introduction

Luminescence dating techniques have been considered an important tool used by archaeologists and researchers all over the world since it is appearance in the 50s (Daniels et al., 1953; Huntley et al., 1985a; McKeever, 1988; Aitken, 1985). For instance, among materials considered for use by thermoluminescence (TL) technique are ancient ceramics (Martini et al., 2001). The dating of archaeological ceramics to determine the time since firing using the TL technique was initially employed by the University of Bern and California in 1960 (Grögler et al., 1960). Furthermore, geological sediments such as terrestrial and marine origin were material under study for TL dating of light-sensitive traps which became more widespread in the 70s and early 80s (Wintle and Huntley,

1982). In 1984 a new method for dating sediments was proposed by David Huntley and colleagues (Huntley et al., 1985b). This method is based on optical dating using optically stimulated luminescence (OSL) becoming a widely used method for directly dating the burial of sediments to find the time of last exposure to sunlight (Huntley et al., 1985a). As a consequence, currently, TL and especially OSL techniques have become important methods for dating mineral grains, quartz, and feldspar, for establishing geochronological frameworks and in a wide range of geomorphic contexts such as aeolian, fluvial, periglacial, and glacial (Duller, 2004; Carobene et al., 2006; Durcan et al., 2015). TL dating of archaeological ceramics was perfected by Aitken in 1985. It consists of determining the cumulative dose from the pottery and the annual dose rate due to external radiation from the site where the

^{*} Corresponding author. Universidad Nacional de San Agustín de Arequipa, Av. Independencia S/N, Arequipa, Peru. *E-mail address*: cgonzaleslo@unsa.edu.pe (C.D. Gonzales-Lorenzo).

pottery was found (Cano et al., 2015a; Mejia-Bernal et al., 2020). The cumulative dose can be determined by two methods as far as the TL is concerned: the additive dose method and the regeneration method whilst for OSL the regenerative method is used. This is possible using quartz grains that were extracted from the ceramic material by chemical methods (Mejdahl, 1982). Another important physical quantity to be considered is the annual dose rate. This is due to natural radiation from radionuclides which includes 40 K, 238 U, and 232 Th, and in the environment and inside the ceramic material. The annual dose rate is determined by the γ -spectroscopy technique. Natural radiation can excite electrons from the valence band, in the crystal structure of the ceramics produces electrons, some of which may be captured in the localized defects in the forbidden band (Mejia-Bernal et al., 2020).

There are other complementary techniques to be used in the dating studies of sediment and pottery materials. Among them, X-ray diffraction allows us to determine which crystalline structures are present in the material to be studied (Young et al., 1977). Among the non-destructive spectroscopic techniques used in the archaeological material chemical composition study, we can mention X-ray fluorescence (XRF) (Luizar Obregon et al., 2018; Freitas et al., 2010). Electron paramagnetic resonance (EPR) spectroscopy is constantly used to monitor paramagnetic species because the analysis of the signals of these species is used as a temperature reference for ceramic firing temperature (Cano et al., 2015a; Mejia-Bernal et al., 2020; Mangueira et al., 2011). It is a method that allows estimating the firing temperature of archaeological materials (Mangueira et al., 2013).

By means of luminescence techniques, archaeological ceramics from different ancient cultures of the world have been studied. Most of these studies are to estimate the age of these important historical pieces (Cano et al., 2009, 2015a; Mejia-Bernal et al., 2020; González et al., 1999; Hood, 2016; Polymeris et al., 2014; Sánchez et al., 2008; Zevallos, 2000; Roque et al., 2004) and to answer the question: when did these cultures develop? Peru is a country that has had a broad diversity of ancient cultures in the past. For that reason, there are different archaeological sites throughout the country that have been discovered and continue to appear today. Among the several studies performed about ancient cultures in Peru (Mejia-Bernal et al., 2020; Zevallos, 2000; Roque et al., 2004; Cano et al., 2009; Vaughn et al., 2014; Aimi et al., 2016; Sanjurjo-Sánchez et al., 2022), an important one corresponds to the architecture and spatial distribution of the Pre-Hispanic Town of Parasca (Polobaya) Arequipa (Zevallos, 2000). Besides, the northern region of Peru has been also studied before, for example, TL dating studies were carried out on ceramics from the Moche culture by Celine Roque et al. (Roque et al., 2004). They have found that the combined studies of cathodoluminescence (CL) and TL were used to select the appropriate thermal treatment for the evaluation of the final equivalent dose resulting in a reduction of age dispersion. On the other hand, Marsh et al. (Marsh et al., 2021) have performed a study comparing radiocarbon vs. luminescence dating of archaeological ceramics in the southern Andes. They have revealed discrepancies across a range of contexts and ages in which ¹⁴C models produce results that agree with expectations based on independent data. The mentioned reasons for disagreement between methods are still unclear, however unstable luminescence sensitivity in samples seems to be an important factor. In this sense, luminescent techniques are an important tool in the dating of sediments and ceramic fragments, however, it must be taken into account that their environment and even human intervention can alter their luminescence response, a fundamental property for determining chronological ages.

Arequipa city is located in the southern part of Peru, in the Andes Mountains. This city is located in a middle-elevation Andean valley between the coastal desert and the high Puna. The central part of the city is crossed by the Chili River from north to southwest, which in its path forms a valley, called the Arequipa Valley or Chili Valley. From the city, it is possible to observe a series of volcanic cones that form snow-capped peaks such as Misti, Chachani, and Pichu Pichu. The weather in Arequipa is usually warm and temperate, due to these reasons and

geographical factors, many cultures have developed in this region of Peru for thousands of years (Cano et al., 2009). Some sites in the Arequipa valley have not been studied and are being lost due to urban expansion and looting in these areas. In these regions, there are two important local cultures: the Churajon, influenced by the Tiwanaku culture, and the Chuquibamba (Mejia-Bernal et al., 2020). In the south region, especially in Arequipa, there are many complexes or archaeological sites, such as Churajon, Maucallacta, Ampato, Uvo Uvo, San Antonio, Yumina, and the most extensive in its time would be Churajon among others, which have been studied by different Archaeologists and Institutions (Mejia-Bernal et al., 2020; Cano et al., 2009; Szykulski et al., 2016; Wasilewski, 2014; Szykulski, 2001). Churajon was the largest pre-Hispanic complex in the south of Peru, covering a large part of Arequipa, being investigated since 1994 by the Catholic University of Santa María (Arequipa, Peru) in collaboration with archaeologists from Poland, who had a great international impact with their contributions, obtaining results for the Late, Middle and Early periods (Wasilewski, 2014; Szykulski, 2001). Vera C. Chavez (Chavez, 2019) has shown an approximation of the reconstruction of the historical process of the Churajon Society from the early period until the Spanish invasion of Peru. Table 1 shows the chronological table of the Central South Andes of Peru. That is the period of the South-Central Andes, Circum Lacustre region, Sub Region North Western Valleys, and also the Central Andes (Chavez, 2019). Besides, this author has mentioned that the Late Churajon period is characterized by vessels that are most often pitchers and glasses, even pots. Pitchers have necks with wider edges that imitate the Inca-style pitchers (Chavez, 2019). It is also worth showing a hypothetical reconstruction of the Churajon village carried out by A.C. Rosas (Rosas, 2002) as shown in Fig. 1. As can be seen in this picture, due to lacking agricultural possibilities due to altitude and temperature, a high livestock potential, has been used by the Churajon Society.

In this work, the age of the ceramic fragments from the Tunata-hill archaeological site is investigated by TL and OSL dating methods to determine the period in which this culture has developed. Furthermore, the firing temperature of ceramic fragments was investigated to know the technology used in the manufacture of their pottery vessels, and thus reconstruct the past of the ancient inhabitants of the southern region of Peru. Our study, based on XRD, XRF, TL, OSL, and EPR techniques to study the ceramics from the archaeological site of Churajón, will be of great help to archaeologists in Peru. With the results of this research, we will be able to understand the chronology and determine the areas of dispersion and density of the archaeological occupation in the Arequipa valley.

Table 1 chronology of the southern region of the Peruvian Andes where the Churajon culture is found (Chavez, 2019).

Age	South Central Andes	Circum Lacustre region	North Sub Region Western Valleys	Central Andes periods
1530	Late Period	Inca	Late Churajon	Late Horizon
1200		Colla,	Middle Churajon	Late
		Lupaca,		Intermediate
		Pacaje		Period
900	Middle	Tiwanaku	Early Churajon	Middle Horizon
	Period			
500	Early	Pucara	Socabaya	Intermediate
	Period			Early Period
0 200				Early Horizon
BC				
3000	Archean			Archean
BC				
10 000	Pre-		Huanaqueros	Pre-Ceramic
BC	Ceramic		Puntillo Sumbay	



Fig. 1. Hypothetical Reconstruction of a Churajón Village (adapted from Rosas, 2002 (Rosas, 2002)).

2. Study area

Tunata-hill archaeological site is an archaeological unit of the Churajón Archaeological Complex that has not been registered by archaeology. Fig. 2a shows a view of Churajón place in a continental view, for a geographical view of this place see Fig. 2b and 2c. According

to Szykulski (2000) (Szykulski, 2000), the central area of the Churajon complex borders to the north with the ruins of Maucallacta, close to Polobaya; south to the Amarcanqui ravine, 4 km south of the Chapi Sanctuary; to the west with the road to the "Cuprita" mine and; to the east it would include the chain of hills that delimit the eastern side from the valley of the Corabaya ravine. Inside this area, the following housing

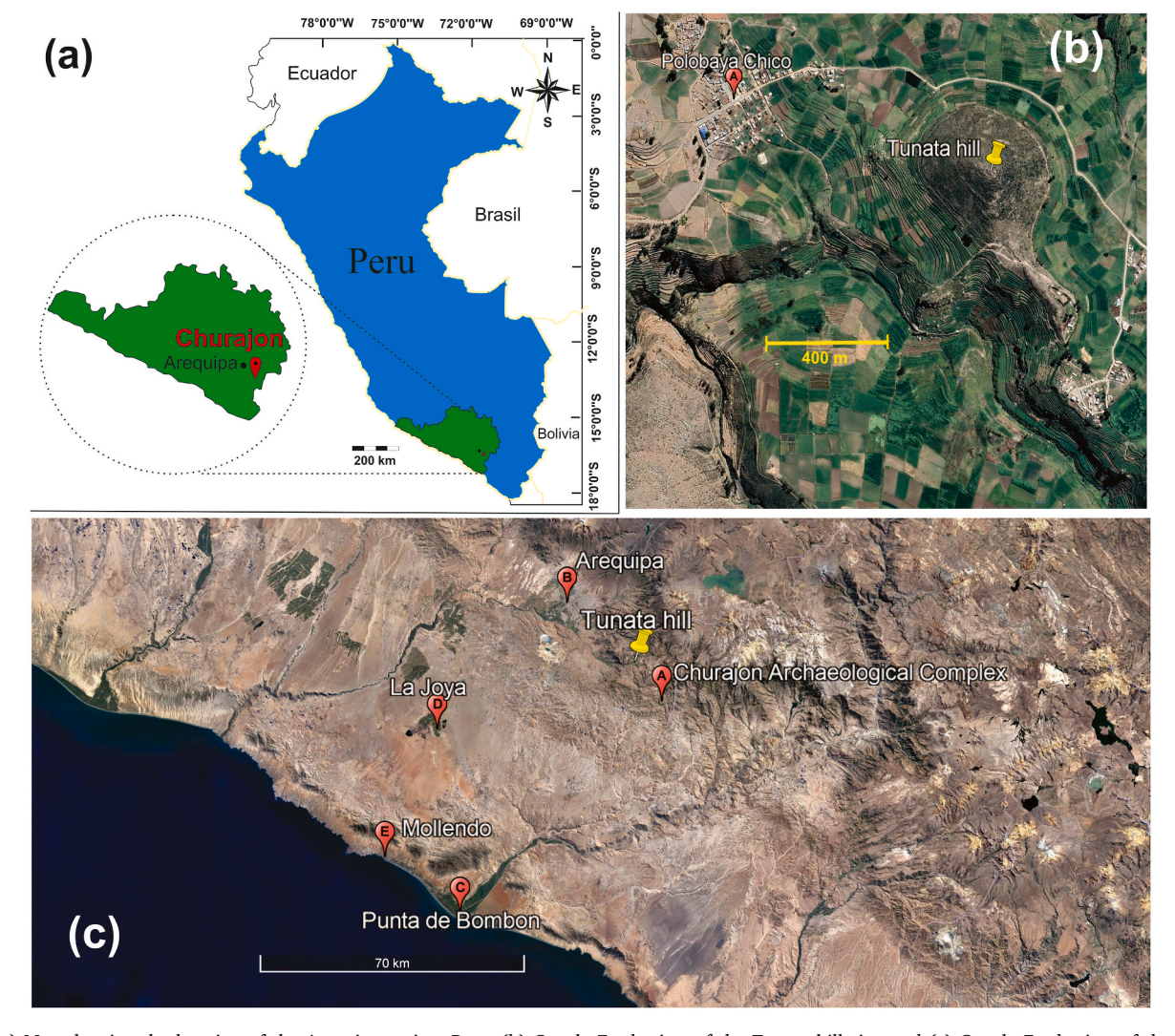


Fig. 2. (a) Map showing the location of the Arequipa region, Peru; (b) Google Earth view of the Tunata hill site; and (c) Google Earth view of the Churajon archeological complex, Arequipa, and other closer cities.

centers stand out: "Torre Ccasa, Gentilar, Mollebaya, Parasca, Wratislavia, and Administrative-Residential, located on the hills, on both sides of the Segache and Corabaya/Tasata ravines" (Szykulski, 2008 p. 181 (Szykulski, 2008)). Likewise, it is estimated that the political limits of the culture and/or kingdom of Churajon were to the north at the Vítor valley and the south as far as the Tambo valley.

The archaeological site known as Tunata-hill is located in the Buenavista annex (UTM 246075E, 8167420N), Polobaya district, province and department of Arequipa, Peru; at 3181 m above sea level and a distance of 23 km in a southwesterly direction from the Churajon administrative-residential Center (see Fig.2b). The site has an approximate area of 30.21 hectares and is mainly made up of a system of platforms established on the slopes of Tunata-hill. The lower terraces are being used with crops of basic agricultural products, while the upper ones have not been affected by agricultural expansion. They are characterized by their retaining walls that reach up to 1 meter in height, built with locally sourced stones of different sizes as can be seen in Fig. 3(a).

At the top of the hill, only four fragmented fulling mills and ceramics scattered on the surface can be seen as shown in Fig. 3 and 4; also, on some upper landings. The sherds correspond to the types called by Neyra (Avendaño, 1990) as Simple-Churajon and Slipped-Churajon; assigned to the Late Intermediate Period (Szykulski (Szykulski, 1996)) corresponding, according to López (López, 2001), to the Churajon phase

(1200-1350 AD). However, everything seems to indicate that this pottery tradition continues until the Late Horizon, as has been verified in the archaeological excavations carried out by Szykulski (Szykulski, 1996) in Sector 1, Trench I and III, where he confirmed the presence of Inca ceramic fragments next to Churajon ceramics.

3. Materials and methods

The archeological samples used in this study were collected by an archeologist from the National Institute of Culture of Peru (INC - *Instituto Nacional de Cultura* by its acronym in Spanish). These ceramics fragments were found at the Churajon archeological site located in Polobaya district, Arequipa region, Peru. The latitude and longitude coordinates of the collected position are 16°33'42.0" S and 71°22'46.0" W, respectively. The location of this position is shown in Fig. 2. And the fragment pottery samples studied in this work are shown in Fig. 4(a). Fig 4(b) shows the ceramic fragments as they were found and collected on the surface of the aforementioned location.

As samples to be analyzed in this work, the two existing and/or representative types of sherds were chosen. First, fragments belonging to the body of a pitcher of the Slipped-type Churajón for thermoluminescence dating and another from a Simple-type Churajon closed vessel (pot) for determining the degree of firing temperature of the sample. As

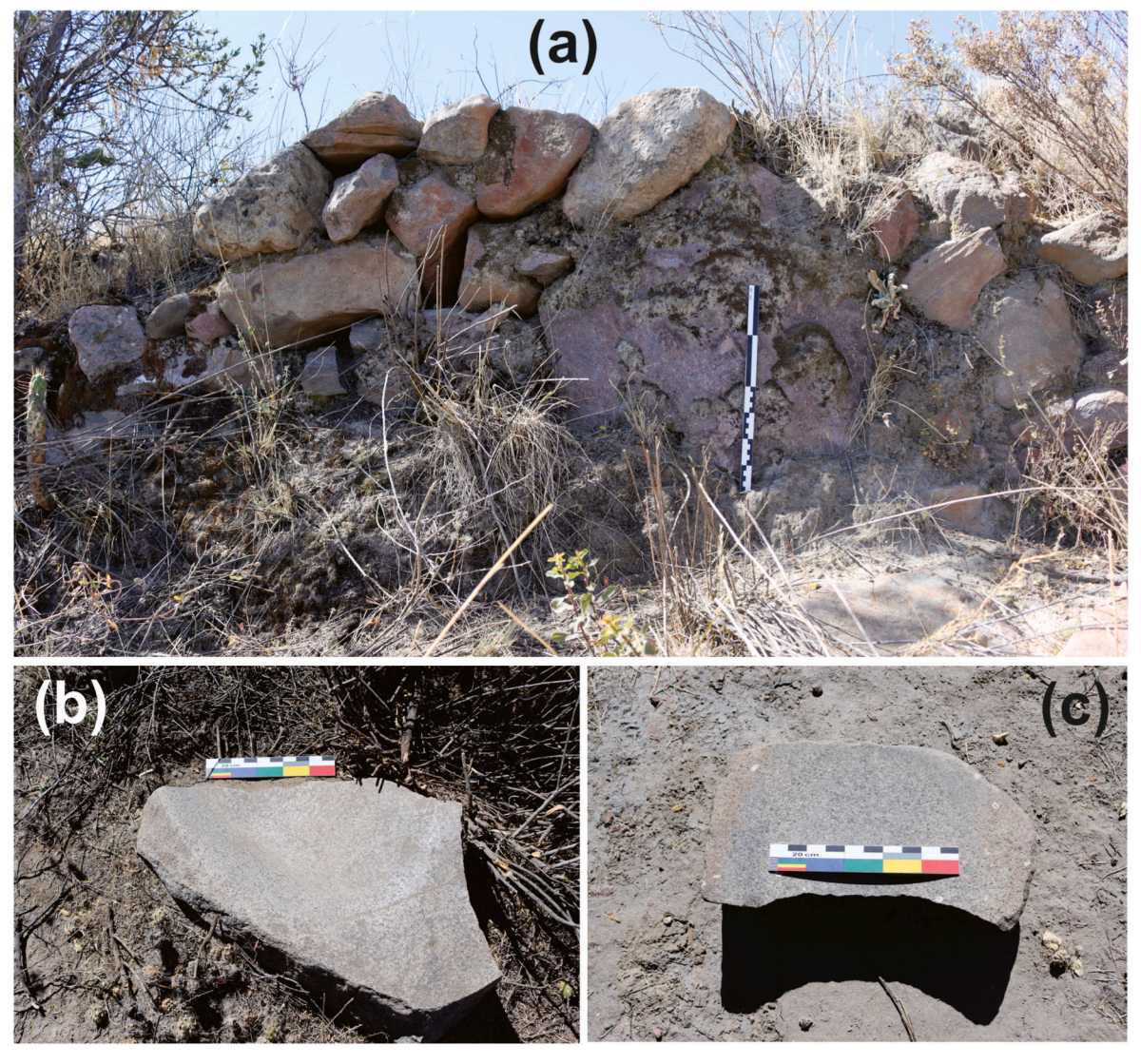


Fig. 3. (a) Picture of a retaining wall and (b-c) fragmented fulling mills found at the Tunata hill site.

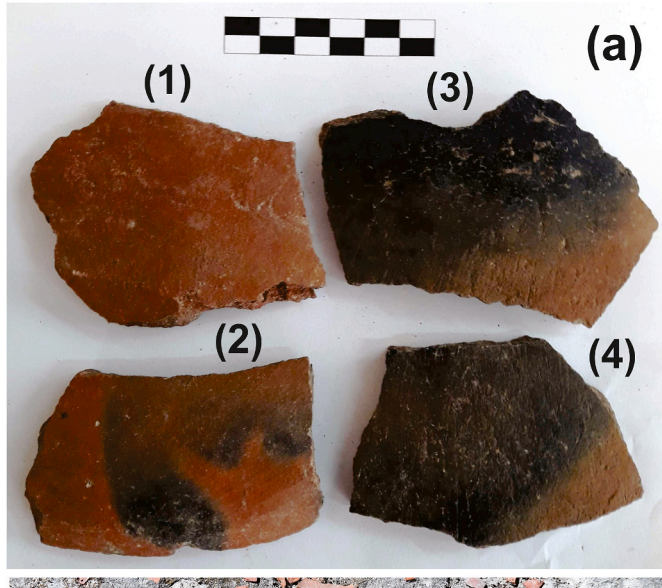




Fig. 4. (a) picture of ceramics fragments collected for dating (1 and 2), XRD analysis (3), and firing temperature determination (4); and (b) ceramics fragments as they were found and collected.

can be seen in Fig. 4(a), the fragment labeled as (1) and (2) are samples used for age determination (Slipped-type); while the fragment labeled as (3) and (4) are the samples used for XRD analysis and firing temperature determination (Simple-type), respectively.

Once the ceramics were in the laboratory, they were cleaned with the help of a toothbrush. The following procedures are based on obtaining the quartz grains from the ceramics collected for luminescence purposes (TL and OSL measurements). For that reason, the outer layer of the ceramic fragments was removed using sandpaper in order to remove any external unknown effect. The obtained cores were carefully crushed first using a hydraulic press and then using a mortar and pestle. The grains obtained were sieved to retain grain sizes between 0.150 and 0.250 mm in diameter and then subjected to a solution of H2O2 for 24 hours to remove organic materials. Thenceforth grains were subjected first to a 25% solution of HF for 30 minutes, to eliminate previous α rays effects and for dissolution of fine grains of feldspar from the sample (Prasad, 2000; Mauz and Lang, 2004). After that, a 10% solution of HCl for 1h to dissolve carbonate minerals was used. After each chemical treatment, previous washing with distilled water was performed to eliminate possible residual chemical solutions. Finally, with a stirrer and a magnet, as much iron as possible was extracted from the sample, and then it was placed in an oven at 75 °C for about 24 hours to dry. All sample preparation was carried out under dim red light to avoid affecting the luminescent signal of the quartz used for TL dating.

A commercial X-ray diffractometer (Rigaku Miniflex 600) equipped with Cu k α 1 radiation (1.5405980 Å) was used to assess the crystal structure of the Churajon sample. X-ray diffraction (XRD) data in the range of 15° \leq 2 θ \leq 60°, with steps of 0.02°, at a rate of 2 °/min were recorded. The XRD patterns were analyzed using the X'Pert HighScore Plus software (Speakman, 2012).

Grains obtained between 0.150- and 0.250-mm diameter were used for TL and OSL measurements, while grains smaller than 0.075 mm in diameter were used in structural X-ray diffraction (XRD) analysis.

For thermal annealing treatment of Churajon samples, a high-temperature oven, model Naberthern GmbH, was used.

Rigaku Supermini 200 WDXRF spectrometer was used to analyze the elemental composition of the Churajon powder sample. Samples were analyzed in a vacuum and referenced to internal standards. Indeed, sample was spread onto a Mylar thin film (Chemplex Industries, Inc.) and elemental analysis F-U was carried out using LiF (200), PET, and RX25 crystals. Afterward, the quantitative analysis was performed through Rigaku ZSX software.

The irradiations for TL measurements were performed at the Professional School of Physics of UNSA (EPF-UNSA) using a Co-60 source from Picker, model Gammatron with a dose rate of 88.23 mGy/min at the point of irradiation. It is important to note that the γ -irradiation was performed at room temperature and under conditions of electronic equilibrium ensuring enough thickness around the sample to avoid electron dose coming from the gamma source on the sample. TL measurements were performed in a Harshaw TL Reader, model 3500, equipped with a photomultiplier tube (PMT) for light detection. The heating rate applied was 4 $^{\circ}\text{C/s}$ in a nitrogen atmosphere.

The reader RISO TL/OSL, model DA-20, from the Department of Marine Sciences of the Institute of Health and Society of UNIFESP - Campus Baixada Santista, was used for OSL readings. The equipment is equipped with blue, green, or infrared light to stimulate the sample, for detection the BG39 filter was used. The reader uses a 9635QA photomultiplier tube. The stimulation wavelength was 830 \pm 10 nm (in the infrared region because the stimulated material was feldspar). This equipment is coupled to a $^{90}\mathrm{Sr}/^{90}\mathrm{Y}$ beta source with an irradiation rate of 0.069 Gy/s for eventual exposure of the studied samples.

The natural radioactive contents from U, Th, and K-40 were determined by γ -spectroscopy, γ -rays spectra of the samples were measured with hyper-pure germanium (HPGe) detector with ultra-low background shield of Canberra Inc.

EPR technique was used to determination of the firing temperature of the ancient fragment pottery. The sample in powder form, without chemical treatment, was divided into 8 aliquots with a mass of 300 mg. Each aliquot of the sample was submitted to different annealing temperatures, from 350 up to 800 $^{\circ}\text{C}$, with an increment of 50 $^{\circ}\text{C}$ using a high-temperature furnace. A Miniscope EPR spectrometer from Freiberg Instruments operating at X-band frequency, 100 kHz modulation, 180 sweet time, 0.2 mT modulation, and 0.5 mW microwave power was utilized for the EPR experiments.

4. Results and discussion

4.1. XRD analysis

The diffractogram for the natural Churajon sample is shown in Fig. 5, all the diffraction peaks of the spectrum coincide with the crystal pattern of the Silicon Oxide SiO_2 identified as (°) and of the Potassium Aluminum Silicate (orthoclase), $K(AlSi_3)O_8$, identified as (*). Both phases are identified with the files 01-085-0794 and 01-075-1190 PDF-2 of the X'Pert HighScore Plus software (Speakman, 2012) for SiO_2 and $K(AlSi_3)O_8$, respectively. The results have shown that 79% of the sample belongs to SiO_2 and 21% to $K(AlSi_3)O_8$. Thus, the SiO_2 structure dominates this sample. Although an HF solution was used for 30 min to dissolve the fine grains of feldspar from the collected pottery, this process was not sufficient to remove it completely. In any case, with the

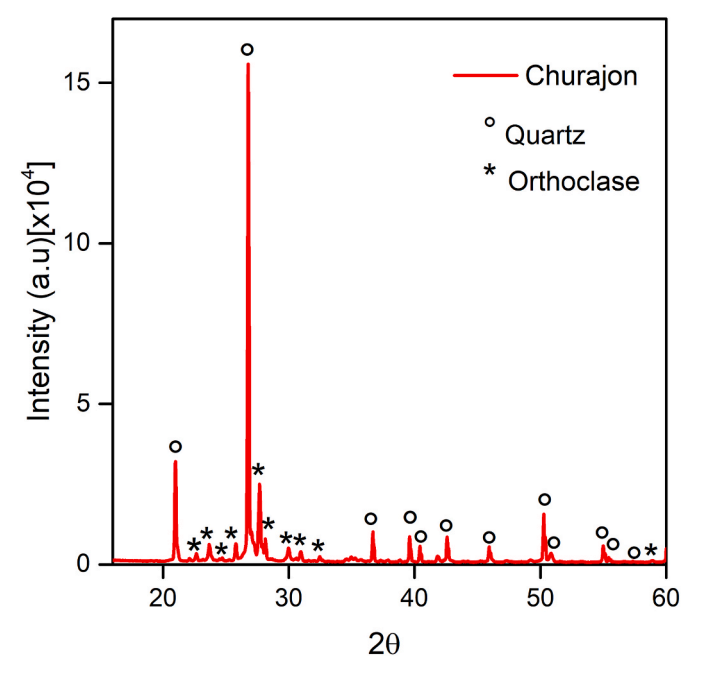


Fig. 5. XRD pattern of the Churajon sample. Two crystalline phases SiO_2 and K K(AlSi₃)O₈ were identified with the files 01-085-0794 and 01-075-1190 PDF-2 of the X'Pert HighScore Plus software (Speakman, 2012), respectively.

chemical treatment carried out on the ceramic samples, the presence of quartz predominates.

3.2. XRF analysis

A study of the elemental composition of ceramics is important to verify the chemical characteristics of the structure of the sediment or clay used for the manufacture of ceramics. Clay gives ceramics the property of being one of the most resistant and abundant materials that can be found in archaeological sites. Therefore, through chemical analysis, we can obtain information about the presence of silicon, aluminum, iron, and other elements that are important for dating and firing temperature determination. The evaluation of the chemical concentration of the pottery powder samples (before chemical treatment) was carried out using the X-ray fluorescence technique (XRF) technique. The values expressed in mass % of the sample (labeled as 3) are shown in Table 2. Table 2 shows that the main constituents of the ceramic paste are Fe (39.5%), Si (30.0%), and Al (10.4%), followed by K, Ca, P and Ti. It is worth noticing from the results obtained from XRF that the Churajon samples are characterized by having a large percentage of Fe (\sim 40%) in their composition. That is why special care is taken to be able to extract iron agglomerates during and after the chemical treatment of the sample as mentioned in Section 2. The presence of a high concentration of Fe agglomerates in the sample extracted after chemical treatment or in the structural composition of the quartz sample can hinder dating by techniques such as electron paramagnetic resonance (EPR) (Ikeya, 1993) since it is known that the EPR signal produced by Fe is intense and overshadows other signals of interest produced by other defects in the crystalline structure for dating. On the other hand, the presence of Fe in the ceramic paste is important for determining the firing temperature of the ceramic. The presence of Si, Al, and K in higher percentages than the other elements in the ceramic is in agreement with the X-ray diffraction analysis, as these elements are the constituents of the crystalline structure of quartz and orthoclase.

3.3. TL studies

In this section, the TL technique was employed to estimate the accumulated dose in the ceramic sherds. TL measurements of natural and irradiated grains obtained from Churajon pottery samples were performed. These grains are composed of quartz together with a smaller amount of feldspar as mentioned before. This makes us careful in selecting the peak that we want to analyze, considering the nature of the appearance of any TL peak. An important study of the TL peaks produced by irradiation of quartz and feldspar composition on silicate minerals was performed by Deokjo Jo and collaborators (Jo et al., 2015). They have shown that the TL glow curves of feldspars samples exposed to gamma radiation, electron beam, and X-ray show a prominent radiation-induced TL peak at 160 °C and a weak high-temperature peak at around 350 °C. On the other hand, quartz irradiated with the same ionizing radiation shows high-intensity TL peaks at around 180, 255, and 350 °C. On the other hand, Mejia-Bernal et al. (Mejia-Bernal et al., 2020) have studied the quartz obtained from ancient pottery from Yumina, Archeological site. The irradiated quartz has shown a high-intensity TL peak at around 250 °C (maintaining a heating rate of 4 °C/s for TL measurements) which was used to obtain Dac-values by the additive method. In this sense, although the feldspar grains have a contribution to the TL intensity, a greater contribution could appear at temperature lower than 200 °C. For this reason, for the regenerative and additive TL method, prior heat treatment of 230 °C for 5 s has been carried out on the grains obtained to eliminate TL peaks below this temperature.

In addition, pottery fading tests (Aitken, 1985) were carried out in the composed grains samples. After laboratory gamma irradiation and after a storage time of 0.33, 1.37, 7.29, 14.3, 21.4, and 27.6 days, TL measurements were performed. Furthermore, before each TL measurement, all samples were heat-treated at 230 °C for 5 s as mentioned before. As a result, after 33 h, the prominent TL peak at about 258 °C shows a decrease of 8% of the maximum TL intensity. After that time, no fading effect has been seen on the TL signal around the peak at about 258 °C. This indicates that the previous heat-treated is suitable to eliminate possible unstable signals and therefore to obtain a reliable result of the accumulated dose after the time of 33 h (all TL measurements were carried out after this time to avoid fading effects).

As a result, TL glow curves obtained are shown in the inset of Fig. 7. The presence of the prominent TL peak is a very broad peak centered at 258 °C that extends from 200 to 400 °C using a heating rate of 4°C/s (inset of Fig. 7). This suggests this broad peak is composed of more than two peaks in this region of temperature. In this situation, the deconvolution process is a usual method used to show the presence of multiple peaks. However, there is a way to avoid the peak deconvolution process which is the Plateau test proposed by Aitken (Aitken, 1985). Aitken has mentioned that for dating purposes a stable region of the TL glow curve should be considered where only traps that have accumulated electrons without leakage are of interest. The plateau test uses a relation N/(N+ β), where N is the *natural* glow curve, and N+ β is the *natural+artificial* glow curve obtained after irradiation. In this work, the plateau test result indicates that any TL peak above the plateau region, from 252 to 325 °C

Table 2Concentration of larger and trace elements obtained by XRF contained in the Churajon powder sample.

Sample	Element (% mass)																	
	Fe	Si	Al	K	Ca	P	Ti	Ba	Mn	Mg	Sr	Zr	Cu	Zn	Rb	S	Cl	Y
Pottery	39.5	30.0	10.4	7,01	5,74	2.24	1.96	1.01	0.485	0.395	0.306	0.275	0.239	0.139	0.131	0.082	0.074	0.012

(circle marked in blue), is suited for dating as can be seen in Fig. 6. The artificial glow curve refers to that of a 30 Gy dose of gamma radiation (from a Co-60 source). Therefore, the TL peak centered at 258 $^{\circ}\text{C}$ was used for dating.

Furthermore, in the present work, to determine the accumulated dose (Dac) by the additive dose method, several aliquots were irradiated at different gamma doses (Co-60 source) from 5 to 50 Gy. The inset of Fig. 7 shows the TL responses of the natural and irradiated samples. For the standard TL multiple-aliquots additive-dose procedure, 40 aliquots were employed (about 8 mg for each aliquot). First, 5 aliquots were used for the measurements of the natural TL signal. To build up the dose-response curve (Fig. 7), the remaining 35 aliquots were used and divided into seven groups of five aliquots. The seven groups were irradiated with doses of 5, 10, 20, 30, 40, 50, and 60 Gy, respectively. After the measurement of the natural signal, the sequence of gamma dosing, preheating, and measuring was repeated to construct a growth curve.

After TL experiments, the peak centered at 258 °C for the glow curves was used to obtain the Dac value by the additive method. Subsequently, the dose-response curve can be built up as shown in Fig. 7. This figure shows the TL intensity response of the 258 °C TL peak as a function of gamma radiation dose. The cumulative dose (Dac) was found by extrapolating the dose-response curve through an adjustment with a linear function (equation of Ikeya), obtaining an accumulative dose of Dac $=1.55\pm0.18$ Gy.

The regenerative method is the other method used by the TL technique in order to verify the result of the accumulative dose value obtained above. The natural quartz grains obtained from the Churajon pottery sample were annealed at 400 °C for 30 min to clear previously natural TL and then irradiated from 5 to 100 Gy of gamma radiation dose (Co-60 source) in the same range used in the additive dose. In addition, before each TL measurement, all samples were heat-treated at 230 °C for 5 seconds to remove TL peaks below 230 °C in a similar way to the additive dose method. As a result, TL glow curves obtained after the mentioned procedure show a broad TL peak of about 262 °C as can be seen in the inset of Fig. 8. This figure also presents the TL intensity as a function of the gamma dose for the regenerative method. Comparing the TL intensity value of the non-annealed natural sample using a straight line as can be seen in Fig. 8, the value of Dac $=1.52\pm0.10$ Gy was

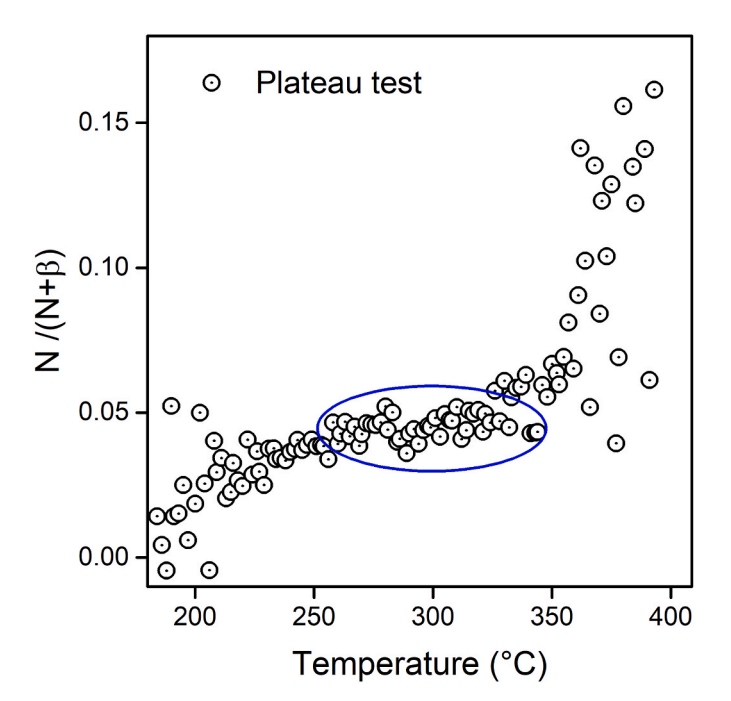


Fig. 6. Plateau test, the ratio of the natural TL intensity (N) and artificial TL (β) for quartz grains from the Churajon pottery sample.

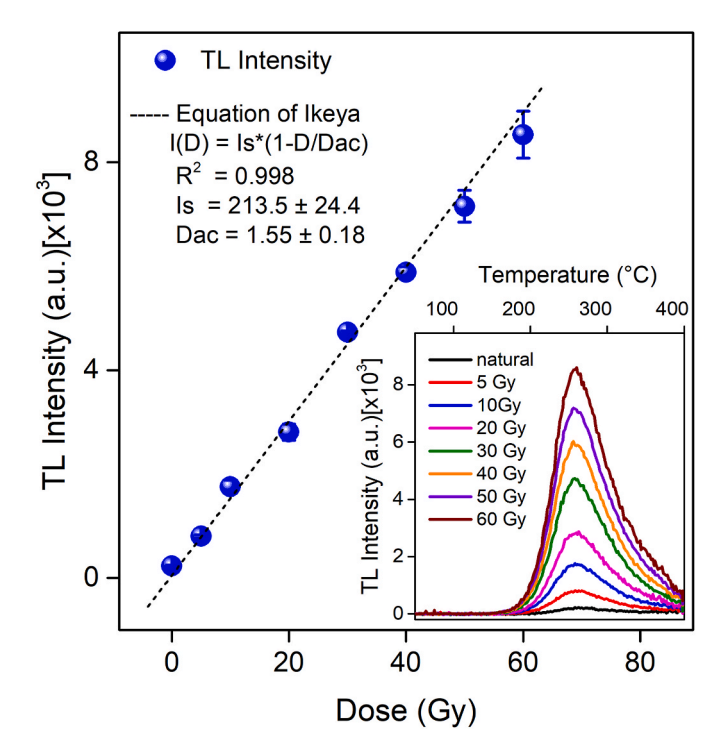


Fig. 7. TL intensity of the 258 °C peak as a function of the dose given to quartz grains extracted from Churajon pottery sample for the determination of Dac. In the inset, TL glow curves of natural quartz grains, obtained from the ceramic samples, plus additional gamma radiation doses up to 50 Gy.

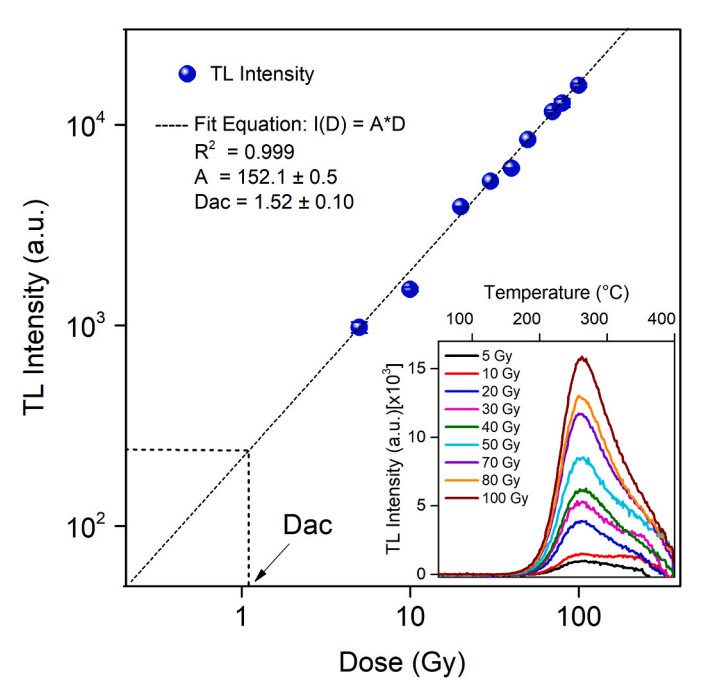


Fig. 8. The behavior of the TL response as a function of the gamma dose of the 262 $^{\circ}\text{C}$ TL peak of the Churajon pottery sample. In the inset, TL glow curves of samples annealed at 400 $^{\circ}\text{C}$ for 30 min and then irradiated to gamma doses indicated in the figure.

obtained. The calibration curves were fitted to a linear equation I(D) = A*D, where D: is the irradiation gamma dose, and A: is the slope of the fitted linear curve.

3.4. OSL studies

Elemental and structural analysis of the ceramic sample showed the presence of potassium aluminum feldspars (KAlSi₃O₈) together with quartz grains (SiO2). Therefore, the stimulation wavelength of the sample was 830 \pm 10 nm, that is, in the infrared region in order to stimulate the feldspar component (Jo et al., 2015; Stokes and Fattahi, 2003; Buylaert et al., 2012). Although the main advantage of using feldspar compared to quartz grains is that the fast component of the OSL signal saturates at higher doses, which allows for determining the age of samples over 150 ky. However, many authors agree that the anomalous fading of the luminescent signal is the main difficulty in finding a reliable age in stimulated infrared luminescence (IRSL) dating of feldspar (Huntley and Lamothe, 2001; Huntley and Lian, 2006; Spooner, 1994). For that reason, several attempts were proposed in order to correct IRSL dating of feldspar such as a measurement of the fading rate in terms of percentage loss per decade; experimental protocol procedures without anomalous fading correction (Lamothe et al., 2003; Roberts, 2012; Li and Li, 2011); and also double (post-IR) OSL signal (Roberts and Wintle, 2001).

In the present work, a pre-heating of 200 $^{\circ}\text{C}$ for 10 seconds was performed on samples after artificial irradiation in order to eliminate unstable signals as well as trying to mitigate the fading effect in age determination by the IRSL technique.

For the accumulated dose determination, a single-aliquot regenerative-dose (SAR) protocol was used (Murray and Wintle, 2000; Murray and Wintle, 2003) measurements were performed at 125 °C during 100 seconds. This protocol is based on measuring a signal after each dose and stimulation cycle, this helps us as a surrogate measure of the sensitivity applicable to the previous measurement cycle. With this procedure, we can verify if the aliquot suffers from sensitivity due to constant irradiation, luminescence reading, and heat treatment in the next measurement cycles. The characteristics of the OSL decay curve were first investigated in terms of behavior in the SAR protocol, dose-response, and dose recovery. As the same aliquot is used for reading and irradiation, it is not recommended to use many irradiations to avoid some sensitivity changes, for regenerative dose was used four points: 0.7, 1.4, 2.1, and 0 Gy, with a test dose of 0.34 Gy, after that, a 200 °C of pre-heating to eliminate unstable signal as mentioned before. The considered values for passing the test were: a zero-dose ratio of less than 2% of the natural ratio $((L_0/T_0)/(L_N/T_N) < 2\%)$, 0 and N are the values corresponding to the zero and natural dose. The error in the equivalent dose, and a recycling ratio of less than 5% $((L_i/T_i)/(L_i'/T_i') < 5\%)$. L_i represents the OSL intensity corresponding to the i-dose, while Ti corresponds to the OSL intensity of the test dose. For the accumulated dose, 47 aliquots were used and 40 aliquots passed all the criteria for SAR tests with a dispersion of 2% within 2σ errors which indicates high internal consistency because the grains were totally reset when ceramics were fired. SAR laboratory growth curve for one of the aliquots and the OSL decay curves can be seen in the inset of Fig. 9 for a single aliquot grain extracted from the Churajon pottery sample. As can be seen in this figure, the growth of the OSL signal with the gamma dose was fitted to a linear equation whose parameters are shown in the mentioned figure. It is important to note that Fig. 9 is a representative example of the luminescence characteristics exhibited by the sample grains with good behavior in the SAR protocol. Finally, Fig. 10 shows the histogram of the distribution of the accumulated dose distribution of sample grains from Churajon pottery adjusted to a normal distribution. This result shows a considerable tight and symmetrical distribution, after the rejection of seven aliquots with low-dose or high-dose outliers considered to be abnormal aliquots. A cumulative dose of 1.54 \pm 0.05 Gy was obtained. Although this result is expected to be overestimated due to fading effect consideration, a result quite similar to that obtained by the additive TL technique is observed.

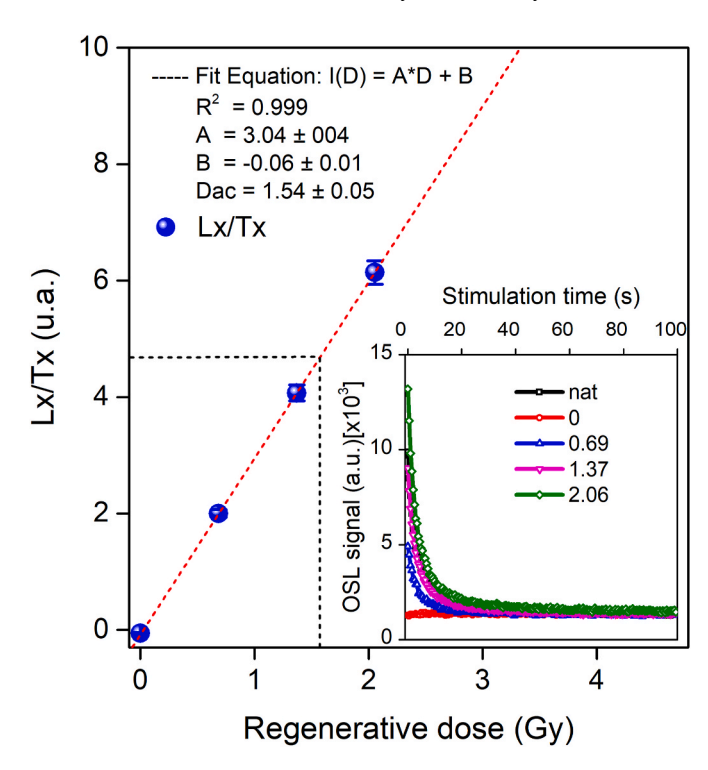


Fig. 9. Representative SAR growth curve for a single aliquot of feldspars grains extracted from Churajon pottery sample for the determination of Dac. The inset shows the OSL decay curves for a single aliquot of feldspars grains.

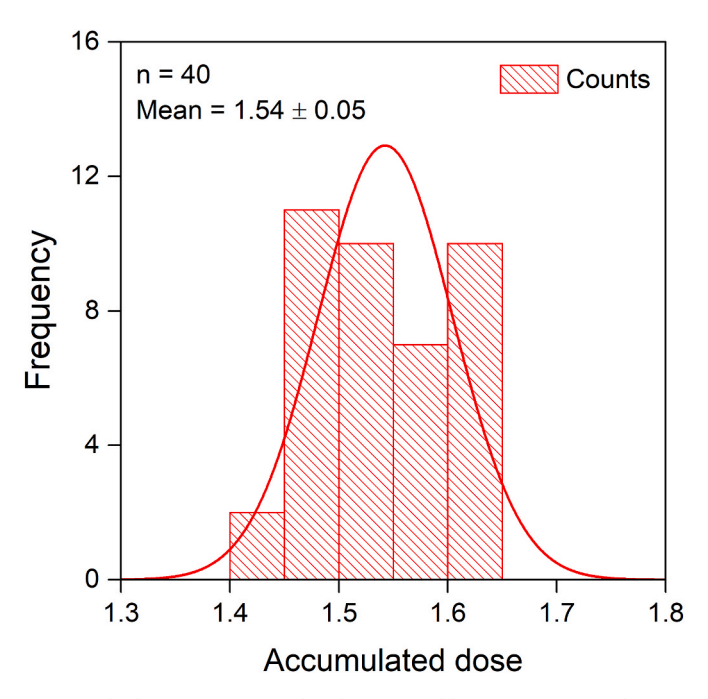


Fig. 10. The histograms of Dac distribution of feldspars grains from Churajon pottery sample for 40 aliquots (n=40).

3.5. Age determination

In this section, after analyzing the TL and OSL results, the natural radiation due to the naturally occurring radioactive elements present within the ceramic fragments collected on the surface and its surroundings sediments has been calculated. The amount of these elements determines the annual dose rate (Dan) at which the quartz or feldspar grains of the ceramic samples were irradiated during the time they were

buried up to the time of dating. For this reason, the $^{232}\text{Th},\,^{238}\text{U},\,$ and $^{40}\text{K}-$ concentrations within the ceramic and of the sediment sample (around the pottery fragment) were measured using the gamma spectroscopy technique as shown in Table 3. The annual dose rate was determined from these concentrations (Ikeya, 1993). Another contribution to the annual dose rate for samples found at surface or shallow burial depth is that due to the contribution of cosmic rays. Hence, in this work, we add the cosmic ray contribution obtained from the equations cited in Prescott and Hutton (Prescott and Hutton, 1988). Thus, the obtained annual dose rate (Dan) value is Dan = 3.113 ± 0.052 mGy/yr. Finally, the age of the pottery can be calculated by Dac divided by Dan (Dac/Dan).

Table 4 shows the accumulated dose (Dac) and age determination of the Churajon ancient pottery by the TL additive, TL regenerative, and OSL methods (determined by the relation mentioned before Dac/Dan). As can be seen in Table 4, the ages found by the TL and OSL techniques are close to each other within the experimental errors. That is, the ages found by both methods are within 1σ of the determined error. The estimated age by additive TL technique is 500 ± 60 yr, that is, the estimated antiquity of this pottery is between the years of 1580 and 1460 AD. Whilst by regenerative TL method is 490 ± 30 yr, that is, the estimated antiquity of this pottery is between the years of 1560 and 1500 AD. By IRSL dating the estimated age is about 490 ± 20 yr (between the years of 1550 and 1510 AD.).

These results are in good agreement due to continuity at the ages found by Kigoshi et al. (Kigoshi et al., 1962) and Szykulski (Szykulski, 1996). These authors found two radiocarbon dates obtained from organic material residues in the Churajón site: The first gives an age of 540 ± 70 yr (Kigoshi et al. (Kigoshi et al., 1962)), and the second date of 570 ± 100 yr (Szykulski, (Szykulski, 1996)). Both dates correspond to the Late Intermediate period (XII-XV century).

Comparing the results of table 4 with the chronology of the southern region of the Peruvian Andes shown in Table 1, it is possible to conclude that Churajon ceramics samples from Tunata-hill belong to the Late Horizon periods (about 1530 AD) which corresponds to the Inca region and the North sub-region of the Late Churajon phase. This phase corresponds to the integration period of the Churajon Society into the Inca Empire and even the beginning of the arrival of the colonizers in America. This integration process can be verified due to the influence of the Inca pottery style on Churajon pottery as mentioned by Cruz (Chavez, 2019). In addition, Chavez (Chavez, 2019) has mentioned that the ceramics found in the Polobaya region corresponds mostly to the Late Churajon phase which would support the results found in the present work. Furthermore, it is possible to say that with the calculated dates and the location where the ceramics were found (at the top of the hill). These pottery fragments possibly belonged to one of the last Churajon villages under Inca rule until the arrival of the colonizers where they began to form a new society.

In this sense, it can be said that the dating of the studied samples in this work, although small, can be an important contribution to regional and national archeology because it would ratify what was indicated by Szykulski (Szykulski, 1996), personifying the continuity of the Slipped-Churajón and Simple-Churajón sherds types, under Inca domination.

3.5. Firing temperature determination

Another critical study considered in this work is the determination of the firing temperature of the fragment pottery labeled as (4) (See

Table 3Concentration of U, Th, and K in pottery and sediment samples used to calculate annual dose rate (Dan).

Sample	²³² Th (ppm)	²³⁸ U (ppm)	⁴⁰ K (%)
Pottery	21.18 ± 0.76	2.79 ± 0.13	2.34 ± 0.07
Sediment	1.7 ± 0.2	0.36 ± 0.07	0.67 ± 0.07

Table 4Accumulated dose (Dac) and age of the ceramics fragments from the Tunata hill site obtained by three different methods.

Method	Dac (Gy)	Age (ky)
TL additive	$1.55 {\pm}~0.18$	0.50 ± 0.06
TL regenerative	1.52 ± 0.10	0.49 ± 0.03
OSL	1.54 ± 0.05	0.49 ± 0.02

Fig. 4a) to decipher the technology used by the inhabitants belonging to this time. These give us important information about the permanence and influence of pottery production techniques among different cultures developed in the region under study. The EPR technique is a physical process involving electronic spin within a magnetic field. When an ionized electron gets trapped due to point defects in a crystalline structure, it forms an atom with an excess of electrons, as well as, an atom with a deficiency of electrons, both with an unpaired electron. These are called "trapped electron" and "trapped hole" centers, respectively, in which they now have a net magnetic moment, μ_e due to the unpaired electron spins. The unpaired electron is detectable with microwave absorption spectroscopy under an external magnetic field. Many studies based on determining the type of electron/hole centers by the EPR technique have been performed in the last decades (Ikeya, 1993; Gonzales-Lorenzo et al., 2020; Callo-Escobar et al., 2022; Cano et al., 2019). As a consequence, an important application of this technique is the possibility to determine the firing temperature of the ceramic sample through successive thermal treatment at high temperatures and where the g-value changes of Fe³⁺ ion indicate the firing temperature of the pottery sample (Bensimon et al., 1998). As indicated by these authors, the EPR measurement parameters, either the EPR intensity or the value of g where the Fe³⁺ ion is found, show a pronounced modification when the heating temperature approaches the annealing temperature. This method is valid even for annealing temperatures greater than 1000 $^{\circ}$ C. This technique has been employed by several authors showing reliable results (Cano et al., 2015a; Mejia-Bernal et al., 2020; Mangueira et al., 2011; Mangueira et al., 2013; Polymeris et al., 2014).

As mentioned above, the analysis of the X-ray fluorescence analysis shows a high percentage of Fe in the ceramic samples, which is an advantage of using the EPR technique to determine the firing temperature. The procedure for this analysis consists of performing successive heat treatments in an increasing manner on the fine powder pottery sample for a constant time. For our ceramic sample, the heat treatment was performed in a preheated kiln in the temperature range from 350 to 800 $^{\circ}$ C. Each sample of about 120 mg was heat-treated for 30 min, then after waiting a reasonable time (at about 2 h) for cooling until it reaches room temperature, EPR measurements were performed. Thermal treatment was performed in a preheated oven. Fig. 11 shows the EPR spectrum of the as-received sample (fine pottery powder), in addition to the samples with previous heat treatment of 350, 550, and 800 °C. A decrease in the EPR intensity is observed when the heating temperature is increased, along with a broad absorption around g = 2. This line is characteristic of Fe agglomerates and the presence of Fe³⁺ in octahedral sites (Cano et al., 2015b). Furthermore, these ions are associated with hydrated species of Fe³⁺ ions, which can be oxidized to FexOy or FeOOH (Bensimon et al., 2000). As mentioned by Bensimon and collaborators (Bensimon et al., 1998), the variation of g indicates a modification of the local symmetry where the Fe³⁺ species is found. This modification causes the value of g to increase or decrease in value due to the widening or narrowing of the EPR line. For the Churajon samples, the value of the factor of g increases as can be seen in the inset of Fig. 11. This figure shows the behavior of the g factor as a function of the firing temperature of the ceramic sample. A sudden variation of the g factor was identified in the temperature region between 500 and 600 $^{\circ}$ C. This indicates that the firing temperature of the ceramic sample is in this temperature range. On the other hand, pottery fragments from the Yumina archaeological complex were dated (827 \pm 30 AD) and their firing temperature

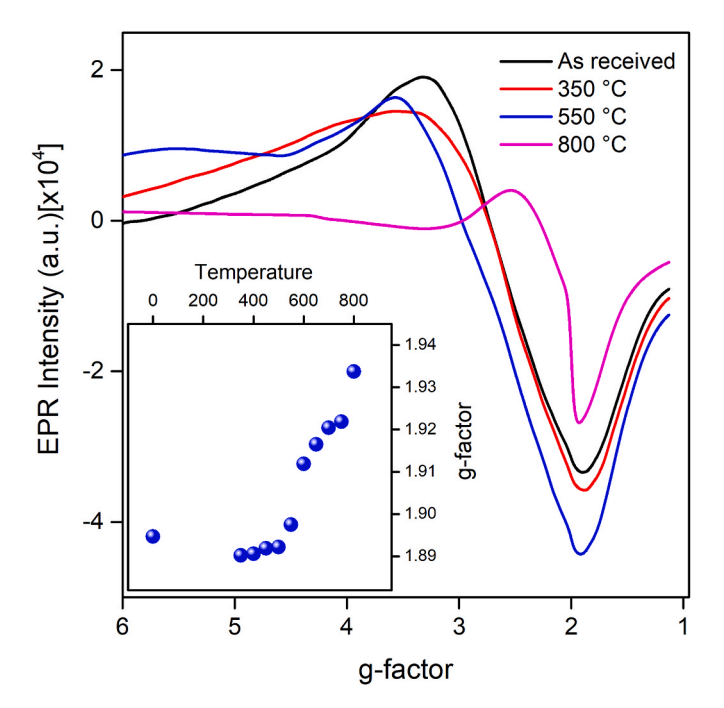


Fig. 11. EPR spectra of ceramic sample powder as received and pre-annealed at different thermal treatments in air. In the inset of the figure is shown the variation of the g-factor of Fe^{3+} as a function of the heating temperature of the Churajon sample (fine pottery powder).

was performed by Mejia-Bernal et al. (Mejia-Bernal et al., 2020). They have found by EPR technique that the firing temperature of ceramics is around 550 \pm 50 °C. These results would indicate that ceramic production technology based on the same firing temperature has been maintained in the southern region of the Peruvian Andes, where the Churajon culture has also developed.

5. Conclusions

The dating of the ceramic sample acquired in the archaeological complex of Churajon-Polobaya, Arequipa, by the additive and regenerative method using the TL and OSL technique reproduced age values close to each other. The age estimated by the additive-dosed TL dating method is 500 \pm 60 years, and 490 \pm 30 years for the regenerative technique. Besides, an age of 490 \pm 20 years was found through the OSL technique. On average, the estimated age by TL and OSL techniques is 490 ± 70 yr, that is, the antiquity of the samples goes from 1600 AD and 1460 AD. These age values belong to the Late Horizon periods which corresponds to the Inca region and the North sub-region of the Late Churajon phase. Besides, periods found corresponds to the integration period of the Churajon Society into the Inca Empire, the fall of this empire, and the beginning of a new society under Spanish colonization. The dating of the samples is a contribution to regional and national archeology because it would ratify the continuity of the Slipped-Churajon and Simple-Churajon sherds types, under Inca domination.

An important conclusion to be indicated in the XRF analysis of the Churajon ceramic (in fine powder) which has shown a high presence of Fe, Si, and Al, followed by K, Ca, P and Ti. The presence of a large percentage of Fe (\sim 40%) in the sample will be an important characteristic in the Churajon ceramics of the aforementioned period.

The analysis of the firing temperature using the EPR signal due to the Fe $^{3+}$ ion indicates that the ancient inhabitants of the Churajon archaeological complex used a furnace that reached a firing temperature of about 550 \pm 50 $^{\circ}\text{C}$ to burn clay and produce their ceramic vessels.

This paper constitutes a step forward in the investigation of the archaeological sites of the valley of Arequipa, but it will be essential in

the near future to add new studies; in particular, to increase the number of samples to confirm the periods in which each sample belongs, and thus, to establish a chronology of the peoples who developed in this region of Arequipa, Peru. It will also be necessary to integrate a characterization of the shapes and geometric figures in the ceramics found so that we can understand their technological development. Another issue that will have to be studied in depth will be the origin and the manufacturing process of the clay used for the manufacture of ceramic vessels.

Author statement

Yolanda Pacompia: Methodology, Investigation, Writing-Original Draft. Justo G. Supo-Ramos: Methodology, Investigation. Carlos D. Gonzales-Lorenzo: Conceptualization, Methodology, Investigation. Darwin Callo-Escobar: Methodology, Software. René R. Rocca: Methodology, Software, Data curation. Elizabeth C. Pastrana: Writing-Review, Visualization. Monise B. Gomes: Writing-Review & Editing, Resources. Betzabel N. Silva-Carrera: Software, Methodology, Validation. S. Watanabe: Methodology, Data Analysis, Validation. Oscar Ayca-Gallegos: Methodology, Validation, Supervision. J. Ayala-Arenas: Project administration, Funding acquisition.

Declaration of competing interest

The authors declare that they have no known competing financial interests or personal relationships that could have appeared to influence the work reported in this paper.

Data availability

Data will be made available on request.

Acknowledgments

This work was carried out with financial support from UNSA-INVESTIGA, Peru (Process number IBAIB-02-2018-UNSA). C.D. Gonzales-Lorenzo kindly acknowledges the financial support from CONCYTEC through its executing unit PROCIENCIA (Contract N° PE501080404-2022-PROCIENCIA, financial scheme E067-2022-04). Besides, the authors kindly acknowledge Prof. Nilo Cano for his important suggestions in the production of this work.

References

Aimi, A., Alva, W., Chero, L., Martini, M., Maspero, F.J.H.S., 2016. Hacia una nueva cronología de Sipán, pp. 129–155.

Aitken, M.J., 1985. Thermoluminescence Dating.

M.N. Avendaño, Historia general de Arequipa, Fundación MJ Bustamante de la Fuente1990.

Bensimon, Y., Deroide, B., Clavel, S., Zanchetta, J.-V., 1998. Electron spin resonance and dilatometric studies of ancient ceramics applied to the determination of firing temperature. Jpn. J. Appl. Phys. 37, 4367–4372.

Bensimon, Y., Deroide, B., Dijoux, F., Martineau, M., 2000. Nature and thermal stability of paramagnetic defects in natural clay: a study by electron spin resonance. J. Phys. Chem. Solid. 61, 1623–1632.

Buylaert, J.-P., Jain, M., Murray, A.S., Thomsen, K.J., Thiel, C., Sohbati, R., 2012.

A robust feldspar luminescence dating method for Middle and Late Pleistocene sediments. Boreas 41, 435–451.

Callo-Escobar, D.J., Cano, N.F., Gundu Rao, T.K., Gonzales-Lorenzo, C.D., Turpo-Huahuasoncco, K.V., Pacompia, Y., Gomes, M.B., Benavente, J.F., Chubaci, J.F.D., Watanabe, S., Ayala-Arenas, J.S., 2022. Identification of ESR centers and their role in the TL of natural salt from Lluta, Peru. Appl. Radiat. Isot. 182, 110126.

Cano, N.F., Arizaca, E.C., Yauri, J.M., Arenas, J.S.A., Watanabe, S., 2009. Dating archeological ceramics from the valley of vitor, Arequipa by the TL method. Radiat. Eff. Defect Solid 164, 572–577.

Cano, N.F., Ribeiro, R.B., Munita, C.S., Watanabe, S., Neves, E.G., Tamanaha, E.K., 2015a. Dating and determination of firing temperature of ancient potteries from São Paulo II archaeological site, Brazil by TL and EPR techniques. J. Cult. Herit. 16, 361–364.

- Cano, N.F., dos Santos, L.H.E., Chubaci, J.F.D., Watanabe, S., 2015b. Study of luminescence, color and paramagnetic centers properties of albite. Spectrochim. Acta Mol. Biomol. Spectrosc. 137, 471–476.
- Cano, N.F., Gundu Rao, T.K., Gonzales-Lorenzo, C.D., Ayala-Arenas, J.S., Javier-Ccallata, H.S., Watanabe, S., 2019. Thermoluminescence and defect centers in synthetic diopside. J. Lumin. 211, 314-319.
- Carobene, L., Cirrincione, R., De Rosa, R., Gueli, A.M., Marino, S., Troja, S.O., 2006. Thermal (TL) and optical stimulated luminescence (OSL) techniques for dating Quaternary colluvial volcaniclastic sediments: an example from the Crati Basin (Northern Calabria). Quat. Int. 148, 149-164.
- Chavez, P.A.C., 2019. La sociedad Churajón: Un proceso de desarrollo local. Facultad de Ciencias Histórico Sociales Universidad Nacional de San Agustin de arequipa.
- Daniels, F., Boyd, C.A., Saunders, D.F., 1953. Thermoluminescence as a research tool. Science 117, 343-349.
- Duller, G.A., 2004. Luminescence dating of Quaternary sediments: recent advances. J. Quat. Sci. 19, 183-192.
- Durcan, J.A., King, G.E., Duller, G.A.T., 2015. DRAC: dose rate and age calculator for trapped charge dating. Quat. Geochronol. 28, 54-61.
- Freitas, R.P., Calza, C., Lima, T.A., Rabello, A., Lopes, R.T., 2010. EDXRF and multivariate statistical analysis of fragments from Marajoara ceramics. X Ray Spectrom. 39, 307-310.
- Gonzales-Lorenzo, C.D., Rao, T.K.G., Cano, N.F., Silva-Carrera, B.N., Rocca, R.R., Cuevas-Arizaca, E.E., Ayala-Arenas, J.S., Watanabe, S., 2020. Thermoluminescence and defect centers in β-CaSiO3 polycrystal. J. Lumin. 217, 116783.
- González, P., Azorin, J., Schaaf, P., Ramirez, A., 1999. Assessing the potential of thermoluminescence dating of pre-conquest ceramics from Calixtlahuaca. Mexico, Radiation protection dosimetry 84, 483-487.
- Grögler, N., Houtermans, F.G., Stauffer, H., 1960. Ueber die datierung von Keramik und Ziegel durch Thermolumineszenz. Helv. Phys. Acta 33.
- Hood, A.G., 2016. Optically Stimulated Luminescence (OSL) Dating and its Application to Ancient Egyptian Ceramics in the 21st Cent.
- Huntley, D.J., Lamothe, M., 2001. Ubiquity of anomalous fading in K-feldspars and the measurement and correction for it in optical dating. Can. J. Earth Sci. 38, 1093-1106.
- Huntley, D.J., Lian, O.B., 2006. Some observations on tunnelling of trapped electrons in feldspars and their implications for optical dating. Quat. Sci. Rev. 25, 2503–2512.
- Huntley, D.J., Godfrey-Smith, D.I., Thewalt, M.L., 1985a, Optical dating of sediments, Nature 313, 105-107.
- Huntley, D.J., Godfrey-Smith, D.I., Thewalt, M.L.W., 1985b. Optical dating of sediments. Nature 313, 105–107.
- Ikeya, M., 1993. New Applications of Electron Spin Resonance.
- Jo, D., Sanyal, B., Lee, J.-W., Kwon, J.-H.R., Chemistry, N., 2015. Thermoluminescence characterization of isolated minerals to identify oranges exposed to γ-ray. e-beam, and X-ray for quarantine applications 303, 297-304.
- Kigoshi, K., Tomikura, Y., Endo, K., 1962. Gakushuin natural radiocarbon measurements I. Radiocarbon 4, 84-94.
- Lamothe, M., Auclair, M., Hamzaoui, C., Huot, S., 2003, Towards a prediction of longterm anomalous fading of feldspar IRSL. Radiat. Meas. 37, 493-498.
- Li, B., Li, S.-H., 2011. Luminescence dating of K-feldspar from sediments: a protocol without anomalous fading correction. Quat. Geochronol. 6, 468-479.
- López, M.H., 2001. Una colección de cerámica de Casapatac-Cacallinca, Arequipa. Boletín de Lima 126, 61-92.
- Luizar Obregon, C., Zamalloa Jara, M.A., Contreras, K., 2018. Elemental analysis of pigments in the ceramic huaco throat-cutter warrior with trophy using X-ray fluorescence spectroscopy. J Journal of the Chilean Chemical Society 63, 4211-4216.
- Mangueira, G., Toledo, R., Teixeira, S., Franco, R., 2011. A study of the firing temperature of archeological pottery by X-ray diffraction and electron paramagnetic resonance. J. Phys. Chem. Solid. 72, 90-96.
- Mangueira, G., Toledo, R., Teixeira, S., Franco, R., 2013. Evaluation of archeothermometric methods in pottery using electron paramagnetic resonance spectra of iron. Appl. Clay Sci. 86, 70-75.
- Marsh, E.J., Korpisaari, A., Puerto Mundt, S., Gasco, A., Durán, V., Radiocarbon, V.S., 2021. Luminescence dating of archaeological ceramics in the southern andes: a review of paired dates, bayesian models, and a pilot study. Radiocarbon 63, 1471-1501.
- Martini, M., Sibilia, E., Croci, S., Cremaschi, M., 2001. Thermoluminescence (TL) dating of burnt flints: problems, perspectives and some examples of application. J. Cult. Herit. 2, 179-190.

- Mauz, B., Lang, A.J.A.T., 2004. Removal of the feldspar-derived luminescence component from polymineral fine silt samples for optical dating applications evaluation of chemical treatment protocols and quality control procedures 22, 1-8.
- McKeever, S.W., 1988. Thermoluminescence of Solids. Cambridge University Press. Mejdahl, V., 1982. Thermoluminescence dating based on feldspars. Nucl. Tracks Radiat. Meas. 10, 133-136, 1985.
- Mejia-Bernal, J.R., Ayala-Arenas, J.S., Cano, N.F., Rios-Orihuela, J.F., Gonzales-Lorenzo, C.D., Watanabe, S., 2020. Dating and determination of firing temperature of ancient potteries from Yumina archaeological site, Arequipa, Peru. Appl. Radiat. Isot. 155, 108930.
- Murray, A.S., Wintle, A.G., 2000. Luminescence dating of quartz using an improved single-aliquot regenerative-dose protocol. Radiat. Meas. 32, 57-73
- Murray, A.S., Wintle, A.G., 2003. The single aliquot regenerative dose protocol: potential for improvements in reliability. Radiat. Meas. 37, 377-381.
- Polymeris, G.S., Kiyak, N.G., Koul, D.K., Kitis, G., 2014. The firing temperature of pottery from ancient mesopotamia, Turkey, using luminescence methods: a case study for different grain-size fractions. Archaeometry 56, 805-817.
- Prasad, S.J.A.T., 2000. HF Treatment for the Isolation of Fine Grain Quartz for Luminescence Dating, vol. 18, pp. 15-17.
- Prescott, J.R., Hutton, J.T., 1988. Cosmic ray and gamma ray dosimetry for TL and ESR. Int. J. Radiat. Appl. Instrum. Nucl. Tracks Radiat. Meas. 14, 223-227.
- Roberts, H.M., 2012. Testing Post-IR IRSL protocols for minimising fading in feldspars, using Alaskan loess with independent chronological control. Radiat. Meas. 47,
- Roberts, H.M., Wintle, A.G.S.R., 2001. Equivalent dose determinations for polymineralic fine-grains using the SAR protocol: application to a. Holocene sequence of the Chinese Loess Plateau 20, 859-863.
- Roque, C., Guibert, P., Vartanian, E., Vieillevigne, E., Bechtel, F., 2004. Changes in luminescence properties induced by thermal treatments; a case study at Sipan and Trujillo Moche sites (Peru). Radiat. Meas. 38, 119–126.
- A.C. Rosas, Arqueología de Arequipa: de sus albores a los Incas, CIARQ, Centro de Investigaciones Arqueológicas de Arequipa2002.
- Sánchez, J., Mosquera, D., Montero Fenollós, J., 2008. TL and OSL dating of sediment and pottery from two Syrian archaeological sites. Geochronometria 31, 21–29.
- Sanjurjo-Sánchez, J., Viveen, W., Vega-Centeno Sara-Lafosse, R., 2022. Testing the accuracy of OSL and pIR IRSL dating of young geoarchaeological sediments in coastal Peru, Ouat, Geochronol, 73, 101382.
- Speakman, S.A., 2012. Introduction to PANalytical X'Pert HighScore Plus V3. 0. MIT Center for Materials Science and Engineering, pp. 1–19.
- Spooner, N.A., 1994. The anomalous fading of infrared-stimulated luminescence from feldspars, Radiat, Meas, 23, 625-632.
- Stokes, S., Fattahi, M., 2003, Red emission luminescence from quartz and feldspar for dating applications: an overview. Radiat. Meas. 37, 383-395.
- Szykulski, J., 1996. El sitio arqueológico Churajón y el problema de su cronología, Andes. Boletín de la Misión Arqueológica Andina 1, 201-220.
- Szykulski, J., 2000. Evidencias arqueológicas de la Época Precerámica y del Período Formativo en Churajón; Sur del Perú, ślaskie Sprawozdania Archeologiczne. Wrocław XLII, 329-354.
- Szykulski, J., 2001. Wieże grobowe (Chullpas) z obszaru kompleksu osadniczego w Churajón-Peru oraz zagadnienie ich periodyzacji. Przegląd Archeologiczny 49, 127-140.
- Szykulski, J., 2008. Arqueología de Churajón, Sur del Perú., Tambo. Boletín de
- Arqueología, vol. 1. Universidad Católica Santa María. Nº, pp. 179–205. Szykulski, J., Lewis, R.T., Wanot, J., Mikocik, Ł., Krajewska, K., Bewziuk, E., 2016. Investigaciones de la Universidad de Wroclaw/Polonia en los valles occidentales del extremo sur del Perú. Tambo Boletín de Arqueología 3, 9–94.
- Vaughn, K.J., Eerkens, J.W., Lipo, C., Sakai, S., Schreiber, K., 2014. It's about time? Testing the dawson ceramic seriation using luminescence dating, southern nasca region, Peru. Lat. Am. Antiq. 25, 449-461.
- Wasilewski, M., 2014. The growing wave: polish archaeological contributions in the New World. Archaeology 6, 167-198.
- Wintle, A.G., Huntley, D.J., 1982. Thermoluminescence dating of sediments. Quat. Sci. Rev. 1, 31-53.
- Young, R., Mackie, P.t., Von Dreele, R., 1977. Application of the pattern-fitting structurerefinement method of X-ray powder diffractometer patterns. J. Appl. Crystallogr. 10, 262-269
- Zevallos, P.J.A., 2000. La Arquitectura y la Distribuion espacial del poblado Prehispanico de Parasca (Polobaya) Arequipa, Facultad de Ciencias Historico Arqueologicas Universidad Catolica de Santa Maria.